Changes in resistance vessels during hemorrhagic shock and resuscitation in conscious hamster model

HIROMI SAKAI,[1,2] HIROYUKI HARA,[1,2] AMY G. TSAI,[1] EISHUN TSUCHIDA,[2] PAUL C. JOHNSON,[1] AND MARCOS INTAGLIETTA[1]

[1]*Department of Bioengineering, University of California, San Diego, La Jolla, California, 92093-0412; and* [2]*Department of Polymer Chemistry, Advanced Research Institute for Science and Engineering, Waseda University, Tokyo 169-8555, Japan*

Sakai, Hiromi, Hiroyuki Hara, Amy G. Tsai, Eishun Tsuchida, Paul C. Johnson, and Marcos Intaglietta. Changes in resistance vessels during hemorrhagic shock and resuscitation in conscious hamster model. *Am. J. Physiol.* 276 (*Heart Circ. Physiol.* 45): H563–H571, 1999.—The unanesthetized hamster dorsal skinfold preparation was used to monitor diameters and blood flow rates in resistance arteries (small arteries, A_0: diameter, 156 ± 23 μm) and capacitance vessels (small veins, V_0: 365 ± 64 μm), during 45 min of hemorrhagic shock at 40 mmHg mean arterial pressure (MAP) and resuscitation. A_0 and V_0 vessels constricted significantly to 52 and 70% of the basal values, respectively, whereas precapillary arterioles (A_1–A_4, 8–60 μm) and collecting venules (V_C–V_L, 26–80 μm) did not change or tended to dilate. Blood flow rates in the microvessels declined to <20% of the basal values. Resuscitation with shed autologous blood (SAB) showed incomplete recovery of A_0 and V_0 diameters even 2 h after resuscitation (71 ± 14% and 81 ± 18%, respectively, of basal value), whereas other vessels did not change significantly. The behavior of A_0 diameter coincided with the incomplete recovery of blood flow rates in all the vessels (ca. 50%) according to Poiseuille's law, and the incomplete recovery of functional capillary density (ca. 75%). Resuscitation with 8% human serum albumin in saline (HSA) tended to show higher levels of A_0 constriction and A_4 dilation and lowered blood flow rates. Resuscitation with SAB restored tissue P_{O_2} 27 ± 10 mmHg after 2 h, which was near control levels (28 ± 5 mmHg), whereas resuscitation with HSA caused tissue P_{O_2} to remain significantly depressed (6 ± 2 mmHg), and flow rates were significantly lower than resuscitation with SAB. These results indicate that response of the A_0 vessels is the crucial determinant of blood flow in the observed area. The constriction of A_0 may help sustain MAP, and constriction of V_0 may enhance blood redistribution from the skin to the vital organs under the hypotensive condition.

feeding artery; vasoconstriction; autologous blood; albumin; microcirculation

IT HAS BEEN SHOWN in some vascular beds that approximately one-half of the total blood pressure drop across the microvasculature occurs in small arteries and large arterioles (5, 43). They are sometimes referred to as the "resistance arteries" in vascular networks of tissues such as the mesentery, pia mater, skeletal muscle, cremaster, and cheek pouch (28), and they contribute significantly to the regulation of peripheral blood flow (6). Small veins or large venules serve primarily as capacitance vessels. Whereas the responses of the arteriolar network has been extensively studied, such studies have focused on the behavior of the smaller vessels, i.e., <50 μm in diameter. However, it has been shown in hypertensive rats that large arterioles and small arteries, and not small arterioles, are responsible for a major increase in total organ vascular resistance (2).

The microcirculation exhibits different but specific physiological responses in each microvessel type, including the resistance vessels (inner diameter 100–1,600 μm) and capacitance vessels (150–250 μm) to the adrenoreceptor agonists, pH, endothelium-derived relaxig factor (EDRF), metabolism, etc. (9, 11, 12, 23). Because these conclusions were derived from studies performed under anesthesia or were inferred from in vitro studies, it is not clear whether such findings would also pertain to conscious animals. Slaaf et al. (37) and Davis (4) studied resistance and capacitance vessels in the intact unanesthetized bat wing preparation, although they studied arterioles <50 μm. Fenger-Gron et al. (10) recently reported the noninvasive measurement of intestinal blood flow in resistance arteries by implanting a catheter and a pulsed Doppler flow probe (outer diameter 500–1,000 μm), where blood flow was estimated under the assumption that vessel diameter did not change during the procedure.

In previous studies from our laboratory dealing with shock and hemodilution using the unanesthetized hamster dorsal skinfold preparation, we found contradictory phenomena: microvascular blood flow decreased significantly even though arteriolar diameters did not constrict enough to explain the decreased blood flow (19, 34). Those studies were carried out with the hamster chamber window model (7) to examine microvascular perfusion in unanesthetized conditions by intravital microscopy (13, 31), in which the glass window was usually implanted on the dorsal skin in such a manner that the diameter of the largest arteriole observed (A_1) is ~60 μm, and that of the largest venule observed (V_L) is ~100 μm (19, 29). To explore the hemodynamics upstream and downstream from the A_1 and V_L vessels, we installed the glass window in such fashion that a paired small artery (A_0, diameter, 156 ± 23 μm) and a small vein (V_0, 365 ± 64 μm) were present in the window. This modified hamster skinfold model was used to study the diameter, blood flow rate, and oxygen tension of A_0 and V_0 vessels in combination with the conventional observation of the downstream microvasculature, during resuscitation from hemorrhagic shock with human serum albumin (HSA) and shed

The costs of publication of this article were defrayed in part by the payment of page charges. The article must therefore be hereby marked "*advertisement*" in accordance with 18 U.S.C. Section 1734 solely to indicate this fact.

autologous blood (SAB). Intravascular oxygen tension measurements were used to determine whether the observed responses were due to local oxygen regulation or mediated through other mechanisms. We selected HSA as a plasma expander that closely reproduces the characteristics of natural plasma. Our aim was to determine whether the behavior of the larger vessels could explain the decreased flow during hemorrhage and its recovery during resuscitation.

MATERIALS AND METHODS

Animal model and preparation. Experiments were carried out in 20 male Syrian golden hamsters of 66 ± 8 g body wt (Simonsen, Gilroy, CA). All animals were housed in cages and provided with food and water ad libitum in a temperature-controlled room on a 12:12-h dark-light cycle. With each rat under pentobarbital sodium anesthesia (100 mg/kg body wt ip, Abbott, North Chicago, IL), the dorsal skinfold consisting of two layers of skin and muscle was fitted with two titanium frames with a 15-mm circular opening and surgically installed as shown in Fig. 1. A location that included a paired small artery and vein was selected. Layers of skin muscle were separated from the subcutaneous tissue and removed until a thin monolayer of muscle including the small artery and vein and one layer of intact skin remained. A cover glass (diameter, 12 mm) held by one frame covered the exposed tissue allowing intravital observation of the small artery (diameter, 156 ± 23 μm) and vein (365 ± 64 μm) which run in parallel. These are the main feeding and collecting vessels in the tissue.

Polyethylene tubes (PE-10, 1 cm; Becton Dickinson, Parsippany, NJ) were connected to a PE-50 tube (25 cm) via silicone elastomer medical tubes (4 cm, Technical Products) and were implanted in the jugular vein and the carotid artery. They were passed from the ventral to the dorsal side of the neck and exteriorized through the skin at the base of the chamber. The patency of the catheters was ensured by filling with heparinized saline (40 IU/ml).

Microvascular observations of the awake and unanesthetized hamsters were performed at least 5 days after chamber implantation to mitigate postsurgical trauma. During the measurements the animals were placed in a perforated plastic tube (inner diameter, 3.8 cm; length, 17 cm), from which the window chamber protrudes, to minimize animal movement without impeding respiration.

A preparation was considered suitable for experimentation if microscopic examination of the window chamber met the criteria of no sign of bleeding and/or edema, and the diameter of the resistance vessel was >130 μm.

All animal studies were approved by the Animal Subject Committee of University of California, San Diego, and the National Institutes of Health *Guide for the Care and Use of Laboratory Animals* [DHHS Publication No. (NIH) 85-23, Revised 1985] principles have been observed.

Resuscitation from hemorrhagic shock. Hemorrhagic shock was induced by bleeding 50% of the blood volume from the carotid artery in 5 min. Systemic blood volume was estimated as 7% of the total body weight. Blood was withdrawn into a heparinized syringe and stored for 45 min at room temperature. It was not refrigerated because of the short period, thus avoiding the need for rewarming before injection and potential complications due to platelet activation at a low temperature. Mean arterial pressure (MAP) was maintained at ~40 mmHg for 45 min through additional withdrawals in the range of 0.2–0.9 ml. Twenty hamsters were hemorrhaged and four hamsters died during the period of hypotension. Survivors were resuscitated with either SAB (n = 8) or 8% HSA (n = 8) in 5 min. The 8% HSA solution was prepared by dilution of 25% HSA solution (Bayer) with saline. Systemic and microhemodynamic parameters and blood gas parameters were evaluated before hemorrhage (baseline), after 50% hemorrhage, before resuscitation, just after resuscitation, and 0.5, 1.0, 1.5, and 2 h after resuscitation. The in situ

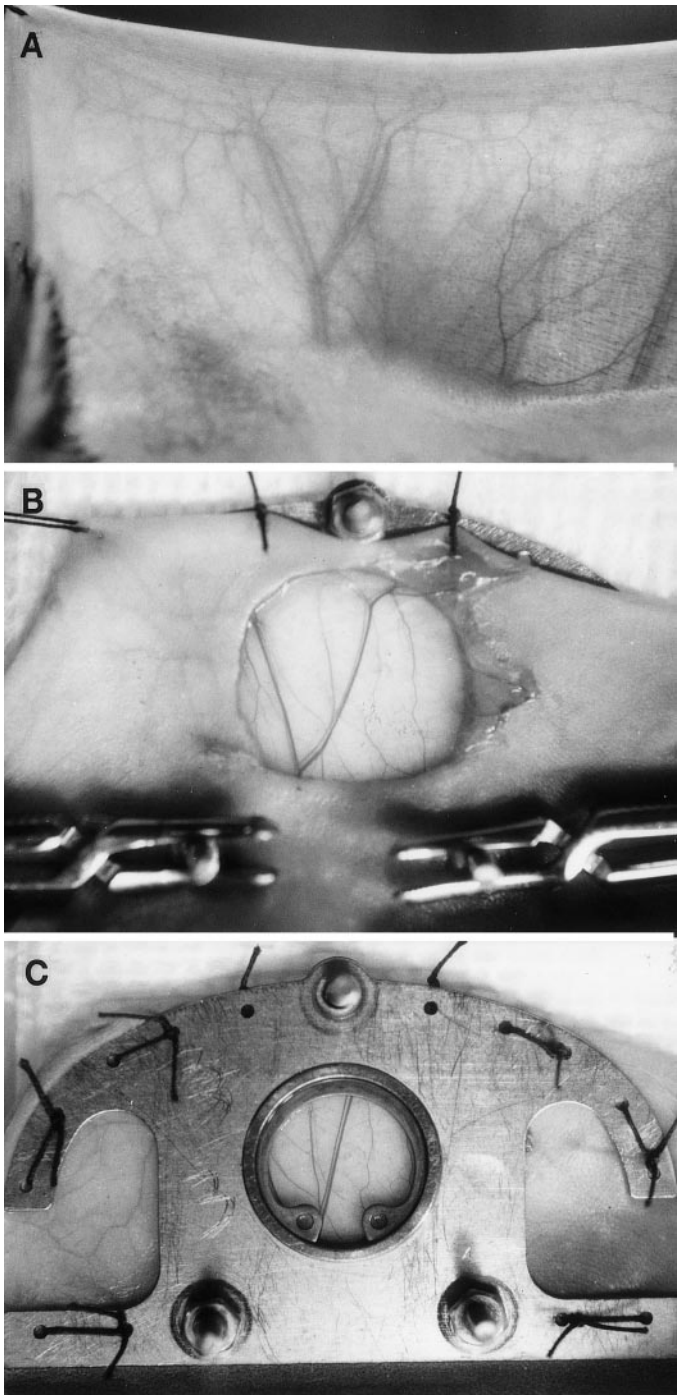

Fig. 1. Surgical procedure of the installation of a glass window on a hamster dorsal skin. *A*: hamster dorsal skin was pulled up to show semitransparently the Y-shaped (sometimes T-shaped) small artery and vein. *B*: layers of skin and muscle on one side were removed until a thin monolayer of muscle and one layer of intact skin remained with the small artery and vein. *C*: cover glass on a frame was installed to the exposed tissue.

microcirculation of the skinfold chamber was observed using a video-microscope system. After 2 h from resuscitation, palladium-porphyrin bound to bovine albumin solution (7.6 wt%, 0.1 ml) was injected intravenously to measure oxygen tension (P_{O_2}) in vessels and interstitium (18, 40).

Characterization of systemic conditions. Blood samples were collected in heparinized microtubes (<100 µl, Curtin Matheson Scientific, Norcross, GA) for hematocrit and blood gas analyses. A pH/blood gas analyzer (model 248, CHIRON Diagnostics, Halstead, UK) was used for analysis of arterial blood oxygen tension (Pa_{O_2}), arterial blood carbon dioxide tension (Pa_{CO_2}), and pH. An analog recording system (Beckman R611, Beckman Instruments, Schiller Park, IL) was used for continuous monitoring of MAP and heart rate (HR).

Microhemodynamic analysis. Microvessels in the subcutaneous tissue and the skeletal skin muscle were observed with an inverted microscope (IMT-2, Olympus, Tokyo, Japan) using a ×10 objective (Olympus) and a ×40 water immersion objective (Olympus, Wplan) and transillumination. Microscopic images were recorded by video (Cohu 4815–2000, San Diego, CA) and transferred to a TV-VCR (Sony Trinitron PVM-1271Q monitor, Tokyo, Japan) and Panasonic AG-7355 video recorder (Tokyo, Japan). Microvessels were classified by their position within the microvascular network according to the previously reported scheme (17). Arteriolar microvessels were grouped into small arteries (A_0, diameter 156 ± 23 µm), large feeding arterioles (A_1, 59.5 ± 11.0 µm), small arcading arterioles (A_2, 25.6 ± 6.4 µm), transverse arterioles (A_3, 10.2 ± 2.5 µm), and terminal arterioles (A_4, 8.6 ± 1.8 µm). Venules were classified as small collecting venules (V_C, 25.9 ± 4.6 µm), large venules (V_L, 79.7 ± 15.3 µm), and small veins (V_0, 365 ± 64 µm). The microvessels selected for measurements were chosen for their optical clarity and not for the nature of their flow. Capillaries and tissue segments selected for measurements were supplied and drained by the arterioles and venules of a functional microvascular unit. These microvessels and capillaries were sketched in advance to plan the sequence of measurements. Selection of vessels in terms of visibility may bias the measurements in the direction of high flow value; however, because the same vessels were measured throughout the study, the trends observed should be representative for the microcirculation in this tissue.

Microvascular diameter and centerline red blood cell (RBC) velocity were analyzed on-line in arterioles and venules (14, 15). Vessel diameter was measured with an image-shearing system (Digital Video Image Shearing Monitor 908, IPM, San Diego, CA), whereas RBC velocity was analyzed by photodiodes and the cross-correlation technique (Velocity Tracker Mod-102 B, IPM). Blood flow rates ($\dot{Q}$) were calculated by means of the following

$$\dot{Q} = (\text{RBC velocity}/R_v)(\text{diameter}/2)^2 \qquad (1)$$

where R_v represents the ratio of velocity in the middle of vessels to whole blood velocity based on the data in the glass tubes. According to Lipowsky and Zweifach (24), R_v equaled 1.6 for larger vessels with diameters >17 µm, and R_v equaled 1.3 for narrower vessels with diameters <10 µm. Therefore, R_v at 1.6 was used for A_0, A_1, A_2, V_C, V_L, and V_0, and R_v at 1.3 was used for A_3 and A_4.

Functional capillary density was analyzed on-line by counting the number of capillaries with RBC flow stemming from one A_3 arteriole, usually ~40–80 capillaries and expressed as a percentage of the basal value.

Determination of microvascular and interstitial P_{O_2}. Subcutaneous microvascular and interstitial P_{O_2} was determined by the method of oxygen-dependent quenching of phosphorescence emitted by bovine serum albumin-bound metalloporphyrin complexes after pulsed light excitation (18, 40). This technique provides a noninvasive measurement of intravascular P_{O_2} and determination of interstitial oxygenation, because intravascularly injected porphyrin complexes bound to albumin extravasate into the interstitium over time. The relationship between phosphorescence lifetime τ and P_{O_2} is given by the Stern-Volmer equation

$$\tau_0/\tau = 1 + k_q \times \tau_0 \times P_{O_2} \qquad (2)$$

where τ_0 and τ are the phosphorescence lifetimes in the absence of molecular oxygen and at a given P_{O_2}, respectively, and k_q is the quenching constant, both factors being pH and temperature dependent. Palladium-*meso*-tetra(4-carboxyphenyl)porphyrin (Porphyrin Products, Logan, UT) bound to bovine serum albumin (Sigma, St. Louis, MO) was diluted with saline to a final concentration of 7.6 wt% (τ_0 = 600 µs, k_q = 325 $\text{Torr}^{-1}\cdot\text{s}^{-1}$, at pH = 7.4, and 37°C) and injected intravenously (0.1 ml). Phosphorescence was excited by light pulse (30 Hz) generated by a 45-W xenon strobe arc (EG&G Electro Optics, Salem, MA), and P_{O_2} measuring sites were microscopically vignetted by an adjustable slit. For intravascular P_{O_2} measurements, the slit was longitudinally fitted within the vessel, whereas for the analysis of interstitial P_{O_2}, it was placed in intercapillary spaces, avoiding interference with blood vessels. Filters of 420 and 630 nm were used for porphyrin excitation and phosphorescence emission, respectively. Phosphorescence signals were captured by a photomultiplier (EMI 9855B, Knott Elektonik, Munich, Germany). In total, 128 decay curves were averaged, visualized, and saved by a digital oscilloscope (Hitachi Oscilloscope V-1065, 100 MHz, Hitachi Denshi, Tokyo, Japan). Decay time constants were determined by computer fitting the averaged decay curves to a single exponential, using the Stern-Volmer equation, and predetermined parameters of τ and k_q were corrected for the prevailing systemic blood pH and temperature (29°C) in the window chamber. Because in anemia pH may be lower than the systemic value and considering that the quenching time constant increases by 8% as pH varies from 7.20 to 6.20, interstitial P_{O_2} may be slightly overestimated.

Microvascular P_{O_2} measurements were made 10 min after dye injection to allow for its uniform dispersion into the vascular compartment, starting with measurements in the vessels, because these initially contain most of the dye. The reflection coefficient for albumin in subcutaneous connective tissue is in the range of 0.8–0.9, causing a natural and continuous steady extravasation of albumin, which yields a measurable steady-state concentration of the albumin-bound porphyrin complex in the tissue within 20–30 min. The material usually appears to be evenly distributed in the interstitium, because there is no evidence of significant variability in signal strength in the interstitium after the initial equilibration of 20–30 min. After the diffusion of the dye, P_{O_2} is not measured in vessels because signals arising from the dye in the overlying tissue may combine with those originating from blood yielding unreliable data. To circumvent this problem, P_{O_2} are measured only once at control and each time point in a hamster group. In the hemorrhage experiments control values were obtained for each group for diameters and blood flow. An additional group of animals (13 hamsters, 68 ± 7 g) was used to obtain the control values for P_{O_2}.

Data analysis. Data are expressed as means ± SD for the indicated number of animals. Data between treatment groups were analyzed using a one-way ANOVA followed by Fisher's protected least significant difference test. A paired *t*-test was used to compare the time-dependent changes within each

group. The changes were considered statistically significant if $P < 0.05$.

RESULTS

Systemic responses. MAP of the SAB and HSA groups before hemorrhage was 99 ± 8 and 102 ± 12 mmHg, respectively, and declined to ~40 mmHg, a level maintained for 45 min (Fig. 2). Immediately after resuscitation, the SAB group recovered to 100 ± 8 mmHg, which tended to gradually decrease to 87 ± 10 mmHg after 2 h, which was significantly lower than the baseline value. The MAP in the HSA group was 58 ± 19 mmHg after resuscitation and slowly rose to a maximum after 1 h to 75 ± 8 mmHg and then tended to decrease. The SAB group had significantly higher MAP than the HSA group at all time points after resuscitation.

In both the SAB and HSA groups, HR significantly fell during hemorrhagic shock. Although the SAB group did not show an immediate recovery, HR returned to 531 ± 91 beats/min after 0.5 h (baseline, 462 ± 78 beats/min). HR in the HSA group did not recover and was significantly lower than in the SAB group after 0.5, 1.0, and 1.5 h.

Hematocrit before hemorrhage was 47–49% and was reduced to ~32% after shock due to the compensatory increase in plasma volume. After resuscitation, the hematocrit in the SAB group increased to 41.8 ± 2.2%, whereas the hematocrit in the HSA group was reduced to 15.7 ± 1.1% due to the dilution with the HSA solution.

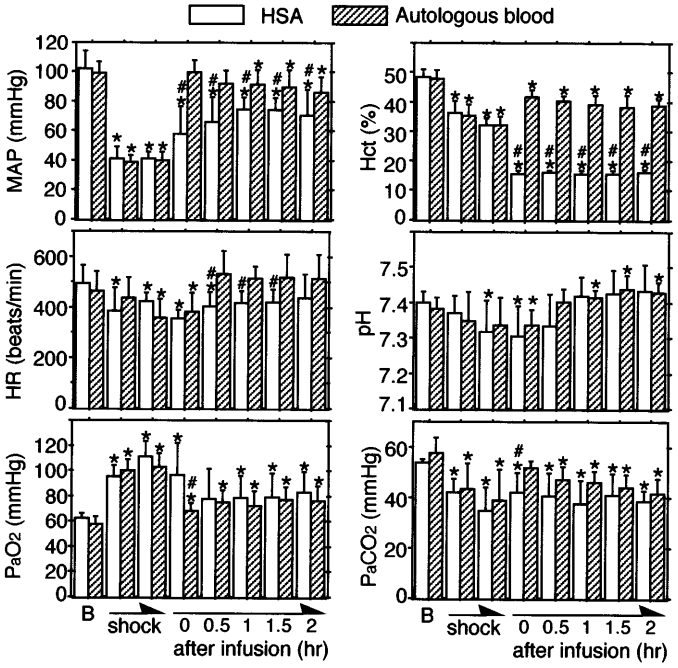

Fig. 2. Changes in systemic parameters from basal values during hemorrhagic shock and after resuscitation with human serum albumin (HSA) or shed autologous blood (SAB). Values are means ± SD. *Significantly different from baseline ($P < 0.05$); #significantly different between two groups ($P < 0.05$). B, baseline; MAP, mean arterial pressure; HR, heart rate; Pa_{O_2}, arterial blood oxygen tension; Pa_{CO_2}, arterial blood carbon dioxide tension; Hct, hematocrit.

Table 1. *Basal values of vessel diameter, centerline red blood cell velocity, and calculated flow rate of observed blood vessels for the experiment and intravascular oxygen tensions in the normal condition*

Microvessels	Diameter, μm	Velocity, mm/s	Flow Rate, nl/s	P_{O_2}, mmHg
A_0	156 ± 23	33.5 ± 7.4	394 ± 133	53 ± 3
A_1	59.5 ± 11.0	10.2 ± 4.4	19.6 ± 13.7	50 ± 3
A_2	25.6 ± 6.4	7.6 ± 4.8	2.52 ± 2.30	47 ± 7
A_3	10.2 ± 2.5	4.5 ± 2.2	0.31 ± 0.24	42 ± 4
A_4	8.6 ± 1.8	2.3 ± 1.1	0.11 ± 0.09	39 ± 5
V_C	25.9 ± 4.6	1.0 ± 0.5	0.36 ± 0.22	33 ± 9
V_L	79.7 ± 15.3	2.9 ± 1.4	9.58 ± 6.11	35 ± 6
V_0	365 ± 64	7.4 ± 2.8	443 ± 216	37 ± 2

Values are means ± SD ($n = 20$ hamsters, 66 ± 8 g body wt for basal values). P_{O_2} measurements were made only once in each group of animals, because they cannot be repeated after the dye has diffused into the tissue; therefore, whereas diameter and blood flow control values could be established for each resuscitation group, control P_{O_2} values were obtained from a separate group of 13 hamsters (68 ± 7 g body wt).

Hamsters in the normal condition at baseline had relatively lower Pa_{O_2} (58.7 ± 5.5 mmHg) and higher Pa_{CO_2} (55.7 ± 3.8 mmHg) than the other animals due to the alveolar hypoventilation, a result from their adaptation to a fossorial environment (30). Hemorrhagic shock induced typical hyperventilation, which significantly increased Pa_{O_2} to 106.1 ± 12.2 mmHg and decreased Pa_{CO_2} to 38.8 ± 9.7 mmHg, and significant metabolic acidosis occurred as shown by the decrease in pH from 7.39 ± 0.03 to 7.33 ± 0.09. The SAB group immediately recovered from the hyperventilation after resuscitation, showing Pa_{O_2} of 68.4 ± 5.9 mmHg and Pa_{CO_2} of 51.8 ± 2.8 mmHg. The HSA showed a decrease in Pa_{O_2}, which was 77.8 ± 23.8 mmHg 0.5 h after resuscitation. Both groups remained slightly hyperventilated after 0.5 h with significant differences in comparison with baseline values. Pa_{CO_2} of the HSA group, however, remained at nonsignificantly lower values than those of the SAB group throughout resuscitation. Both groups tended to increase pH to >7.40, indicating respiratory alkalosis.

Characteristics of classified microvessels. Table 1 shows the basal value of diameter, centerline RBC velocity, blood flow rate, and P_{O_2} of each microvessel. A_0 and V_0 showed centerline RBC velocities of 33.5 ± 7.4 and 7.4 ± 2.8 mm/s, respectively, and blood flow rates of 394 ± 133 and 443 ± 216 nl/s, respectively. P_{O_2} in A_0 was 53 ± 3 mmHg, decreasing to 39 ± 5 mmHg in A_4 arterioles. This reduction is due to the diffusion of oxygen from arterioles (13). Mean P_{O_2} in venules increased slightly from 33 ± 9 mmHg in V_C to 37 ± 2 mmHg in V_0 due to the presence of convective and diffusive oxygen shunts.

Microhemodynamic responses. The hemorrhagic shock period in both the SAB and HSA group induced significant constrictions of A_0 (52% of the basal value), A_1 (82%), and V_0 (70%) and a tendency for dilation of A_2 (104%) and A_3 (117%) (Fig. 3). A_4, V_C, and V_L did not show specific diameter changes. The micrographs in Fig. 4 illustrate vasoconstriction of a small artery and

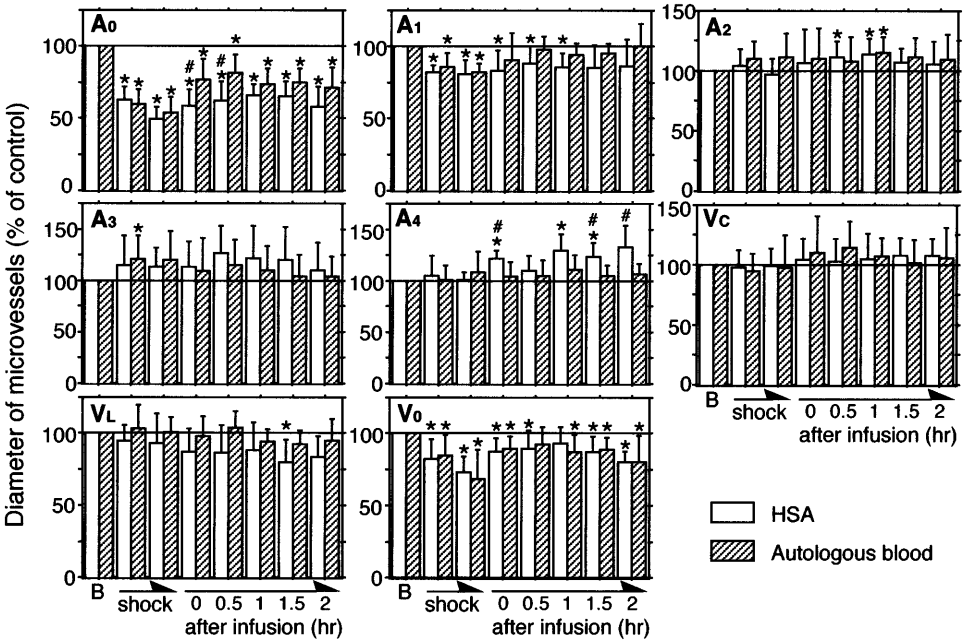

Fig. 3. Changes in diameter of small artery (A_0) and vein (V_0), arterioles (A_1, A_2, A_3, A_4), and venules (collecting and large, V_C and V_L, respectively) from basal values during hemorrhagic shock and after resuscitation with HSA or SAB. Values are means ± SD. B, baseline. * Significantly different from baseline ($P < 0.05$); # significantly different between two groups ($P < 0.05$).

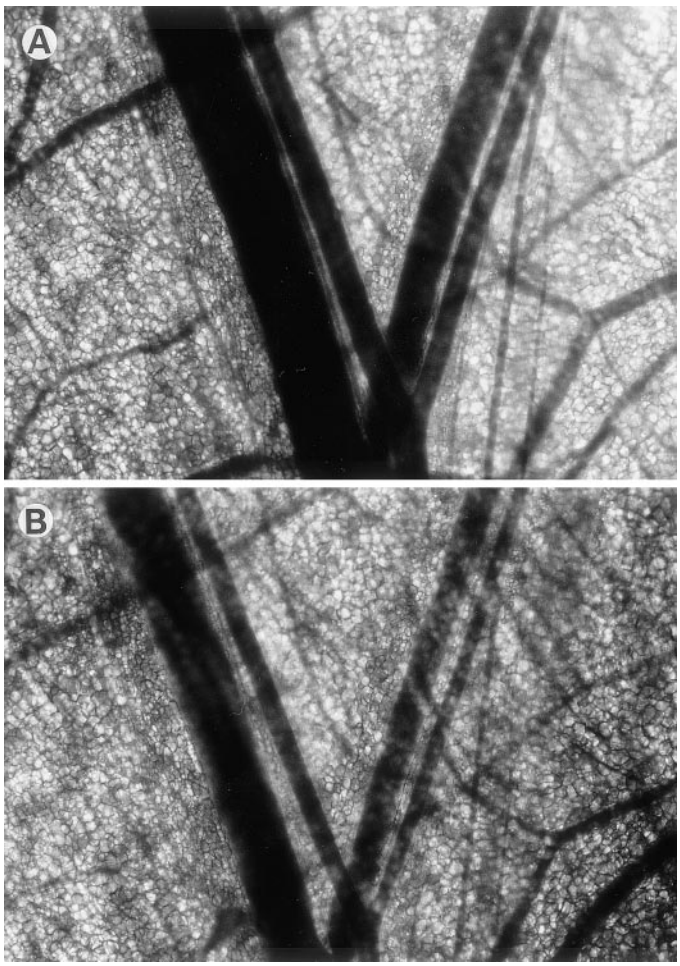

Fig. 4. Micrographs of a set of small artery and small vein before (*A*) and after (*B*) 45 min of hemorrhagic shock, indicating that these vessels significantly constricted.

vein pair. After resuscitation, the diameter of A_1 vessels in the SAB group returned close to the baseline value, and it was not statistically different from control, whereas the diameters of A_0 and V_0 did not return to the basal values and remained significantly lower even after 2 h (A_0, 71 ± 14%; V_0, 81 ± 18%). A_2 and A_3 tended to remain dilated with a significant dilation of A_2 at 1 h (115 ± 13%), whereas A_4, V_C, and V_L microvessels did not show specific changes after SAB infusion. There was a significantly smaller recovery of the A_0 diameter in the HSA group after resuscitation (59 ± 11%) than in the SAB group at 0 and 0.5 h and a tendency to maintain more constriction than in the SAB group; the vessel remained <70% of baseline even 2 h after resuscitation. Both A_1 and V_L tended to maintain constriction at 86 ± 19% and 83 ± 15% of baseline, respectively, at 2 h and with significant constriction of V_L at 1.5 h (80 ± 16%). A_2 and A_3 tended to remain dilated, showing significant dilation of A_2 at 0.5 and 1 h. A_4 dilated after HSA infusion and were significantly larger than basal values at 0, 1, and 1.5 h and significantly larger than the SAB group at 0, 1.5, and 2 h (133 ± 21% at 2 h). V_C did not show significant diameter changes. V_0 did not return to the basal values and remained significantly constricted at 2 h (80 ± 7%).

Although diameter changes were heterogeneous, flow in all the vessels showed similar and significant decreases during the hemorrhagic shock period (Fig. 5) in A_0 (5% of the basal value on the average), A_1 (7%), A_2 (12%), A_3 (7%), A_4 (17%), V_C (8%), V_L (10%), and V_0 (8%), which increased after infusion of the resuscitating fluids. The SAB group showed generally higher recovery in blood flow, e.g., at 0 h in A_0 (SAB 47% vs. HSA 8%), A_1 (32% vs. 22%), A_2 (83% vs. 48%), A_3 (55% vs. 18%), A_4 (90% vs. 75%), V_C (54% vs. 22%), V_L (56% vs. 32%), and V_0 (56% vs. 31%), with significant differences at the following time points: A_0, all the time points; A_1,

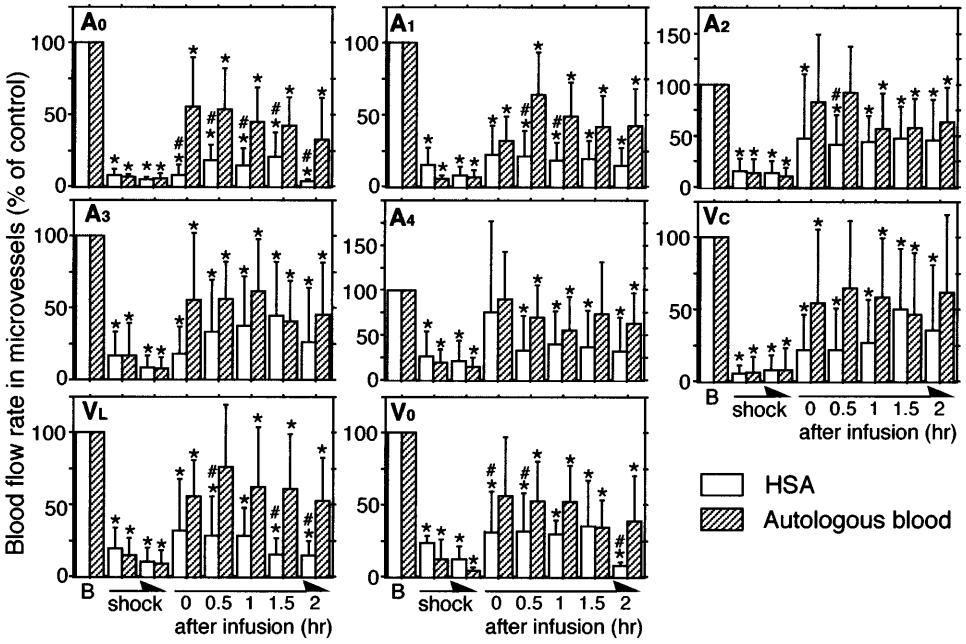

Fig. 5. Changes in blood flow rates in small artery (A_0) and vein (V_0), arterioles (A_1, A_2, A_3, A_4), and venules (V_C, V_L) from basal values during hemorrhagic shock and after resuscitation with HSA or SAB. Values are means ± SD. *Significantly different from baseline ($P < 0.05$); #significantly different between the two groups ($P < 0.05$).

0.5 and 1 h; A_2, 0.5 h; V_L, 0.5, 1.5, and 2 h; and V_0, 0, 0.5, and 2 h. However, flow in the SAB group on the average did not recover to the basal values even after 2 h.

Functional capillary densities of both the SAB and HSA groups diminished after the hemorrhagic shock period to 18% of the basal values (Fig. 6). The SAB group showed an immediate recovery to 75 ± 15% at 0 h, whereas the HSA group was 25 ± 21% and remained below 40% throughout the observation period. Both groups remained at significantly smaller values than the baseline.

Intravascular and interstitial oxygen tensions of the SAB group were nonsignificantly lower than the basal values, except in V_L, although significantly higher than the HSA group except for A_0 vessels. However, intravascular total oxygen content of A_0 of the HSA group was significantly lower than that of the SAB group due to the significantly lower hematocrit (16%); consequently the reduction of downstream P_{O_2} was significant.

DISCUSSION

One of the principal findings of this study is that only small arteries with diameters of ~160 μm and veins of ~370 μm constrict significantly with hemorrhage and remain significantly constricted during resuscitation in the nonanesthetized, intact hamster window preparation. These vessels correspond to branches of the circumflex scapula artery and vein in humans (8) and are located outside of both the skin and muscle. The same kind of vessels in the hamster cremaster muscle and the rat hindlimb muscle preparations were termed "feed arteries" and were reported to regulate blood flow to a significant degree (36, 44). Meininger et al. (27) studied the anatomic arrangement, pressure distribution, and resting vascular tone of feed arteries located upstream from the rat cremaster microcirculation and demonstrated that small arteries of ~140 μm in diameter showed the largest pressure drop of any vascular order.

These blood vessels occupy a special niche within the vasculature in terms of their experimental access, because they are too small to be analyzed by conventional systemic hemodynamic techniques, and con-

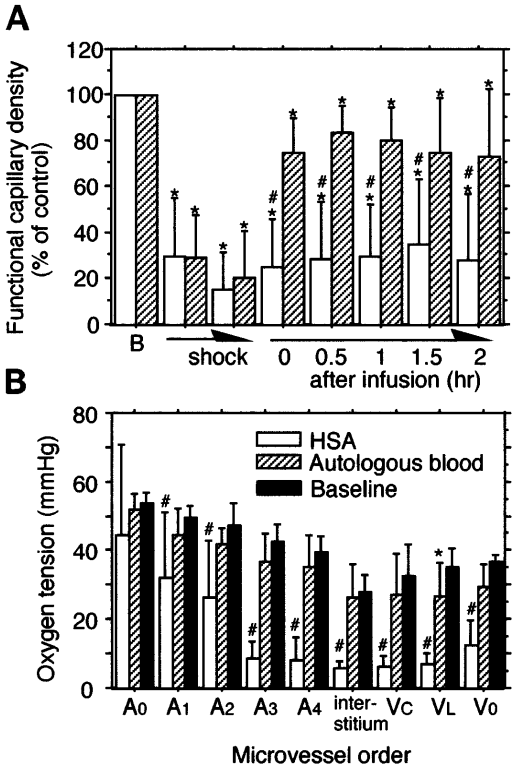

Fig. 6. *A*: changes in functional capillary density from basal values during hemorrhagic shock and after resuscitation with HSA or SAB. Values are means ± SD. *Significantly different from baseline ($P < 0.05$); #significantly different between two groups ($P < 0.05$). *B*: intravascular and interstitial oxygen tensions 2 h after resuscitation in comparison with basal values. #Significantly different from the baseline and SAB group ($P < 0.05$); *significantly different from baseline ($P < 0.05$).

versely they tend to be outside the scope of most microvascular studies and methods. Most previous reports dealing with resistance arteries focus on their reactivity in terms of diameter changes; however, in the hamster skinfold preparation, the tissue is sufficiently transparent to allow measurement of RBC velocity with photodiodes and the cross-correlation technique. Blood flow velocity in these small arteries under normal conditions was 33.5 ± 7.4 mm/s (among the fastest velocity measured with the cross-correlation method) corresponding to a blood flow rate of 394 ± 133 nl/s.

Volume flow in the tissue under study fell to 5–17% of control levels when arterial pressure was reduced to 40 mmHg. This large reduction in flow is in part due to the low MAP and the decline in cardiac output as evidenced by the decreased vascular volume and HR. We were unable to measure cardiac output of the hamsters due to the small body weight (60 g). Cardiac output is reported to fall as much as 50% in hemorrhage (22, 32, 35); however, it is unlikely that it would be reduced to <20% of control, therefore, the decrease in flow in this tissue evidences a significant redistribution of vascular resistance, attributable to the changes in vascular diameter observed in the small arteries and to a lesser degree in the small veins. This suggests that the "centralization" of blood flow in hemorrhage may be controlled by these resistance vessels.

The finding that small arteries and veins are the principal effectors of increased vascular resistance in shock and/or extreme hemodilution explains previous findings from this laboratory showing the significant reductions of blood flow in the absence of notable changes in microvascular vessel caliber. The difference in response between large and smaller microvessels during hemorrhagic shock has been reported in previous studies (3, 17, 19), which found significant constrictions of large arterioles and dilation of precapillary arterioles in conscious hamster dorsal skin. A similar result was found when MAP decreased in the anesthetized and exteriorized cat sartorius muscle (39) and rat cremaster muscle (46). In general, however, the level of constriction found in the larger arterioles was not sufficient to explain the significant reduction of blood flow, suggesting that more significant changes may occur in larger vessels.

Our findings fully support the contention that during hemorrhagic shock, active regulation occurs primarily at the level of the small A_0 arteries and the small V_0 veins. Furthermore, our results demonstrate that interpretation of microvascular events is critically linked to information about the hierarchical distribution of microvessels in the network. In our study, network location fully accounts for the heterogeneous microvascular responses, and vessel reactions follow a defined pattern. As an example, the arcading arterioles A_2 tended to remain at basal values or dilated at all time points after resuscitation from hemorrhagic shock, whereas A_0 and V_0 vessels did not return to the basal value even after resuscitation with SAB.

The time course of change in blood flow in all microvessels and that of functional capillary density, which were significantly reduced during the shock period and increased after resuscitation, also coincided with the diameter changes of the small A_0 arteries and not the remainder of the arteriolar vessels. The SAB group showed higher and faster responses than the HSA group. In terms of Poiseuille's law, blood flow in a tube is proportional to the fourth power of the radius, the pressure gradient, and inversely proportional to fluid viscosity. Assuming that A_0 dominates the downstream blood flow and considering a reduction of A_0 diameter to 80% of the basal value, the reduced blood viscosity due to the reduced hematocrit (ca. 40% for the SAB group, initially 50%), and the reduced MAP, which may affect the regional arteriovenous pressure difference (ca. 90%), then the reduction in blood flow rate can be estimated to be $(0.8)^4 \times 50/40 \times 0.9 \times 100 = 46\%$ of the basal value. This estimate corresponds to our finding on the incomplete recovery of blood flow rates of the SAB group shown in Fig. 5. This calculation indicates that the reactivity of the A_0 small arteries is crucial in determining conditions in the downstream microcirculation.

Normally intravascular P_{O_2} decreases from A_0 (53 ± 3 mmHg) to A_4 (39 ± 5 mmHg). This reduction is due to oxygen diffusion from arterioles and consumption by the vascular wall (13, 41). Tissue P_{O_2} is 28 ± 5 mmHg and blood P_{O_2} increases after passing through the capillaries being 33 ± 9 mmHg in V_C and 37 ± 3 mmHg in V_0 due to the presence of diffusive and convective shunts between arterioles and venules. Two hours after resuscitation, P_{O_2} in vessels of the SAB group were not significantly lower than basal values, although blood flow was reduced and were significantly higher than the HSA group in A_2, A_3, A_4, V_C, V_L, and V_0 vessels. P_{O_2} in A_0 vessels of the HSA group was 44 mmHg, whereas most of the oxygen exited the arterioles before blood entered the capillaries. The low intravascular P_{O_2} values are also a consequence of the decreased blood oxygen-carrying capacity due to the low hematocrit and the diffusion from arterioles before blood enters the capillaries. This phenomenon may be enhanced by the reduced blood flow rate, which may provide additional time for oxygen to diffuse from RBCs to the vascular walls. As a result, P_{O_2} values in A_3, A_4, V_C, and V_L are <10 mmHg on the average.

Our finding may in part be due to nonuniformity of the sympathetic innervation in small arteries and arterioles (12). Normally, α_1-receptors are located only in larger arterioles and venules, and α_2-receptors are located throughout the arteriolar and venular microvasculature (9). The primary compensation to acute hemorrhagic shock includes release of adrenal catecholamines, although norepinephrine (α_2-receptor agonist)-mediated constriction of small terminal arterioles is reduced by a metabolic acidosis (26) and hypoxia (23). In cat sartorius muscle, the escape from sympathetic stimulation is due to a fall in parenchymal cell P_{O_2} and not periarteriolar P_{O_2} (1). Dilation of small arterioles in the hamster cheek pouch during systemic hypotension was reported to be abolished by elevated suffusate P_{O_2} (25). These observations suggest that the escape from

constriction of small arterioles during hemorrhagic shock and resuscitation, such as A_4 vessels in the HSA group, may be due to the impaired oxygenation of the microvasculature as shown by the significantly lower P_{O_2} levels throughout the microvessels in the tissue. Furthermore, the prevalent constriction of the A_0 vessels during shock and resuscitation should reduce hydraulic pressure in the subsequent vessels, which may tend to dilate according to myogenic responses (16). Consequently the lack of constriction in the smaller vessels may be due to the combined effect of two local autoregulatory processes that oppose the constrictor stimulus.

The difference in the recovery of blood flow, oxygenation, and functional capillary density between HSA and SAB may not only be due to oxygen content but also due to the viscosity of the circulating blood and the heterogeneous shear stress-dependent production of EDRF. Griffith et al. (11) showed that rabbit ear small arteries (diameter range: 150–700 μm), where resistance and shear stress are maximal, have the highest EDRF sensitivity. EDRF-mediated shear-induced dilation of arterioles and small arteries has been extensively studied (21, 33, 38). Shear stress on the wall is given by $(4 \cdot \eta \cdot \dot{Q})/(\pi r^3)$, where η is viscosity, $\dot{Q}$ is blood flow rate, and r is the radius. Blood viscosity was determined with a capillary viscometer (42) requiring only a 0.4-ml sample for measurements at an average shear rate of 119 s^{-1}. Circulating blood viscosities after infusion of autologous blood and HSA were 4.0 and 1.6 cP, respectively (intact blood: 4.5 cP). This would reduce shear stress in A_0 arteries by 50% during resuscitation in the SAB group and 90% in the HSA group if the diameter is maintained and may be related to the significant differences in A_0 vessels diameters (45) and functional capillary density between groups.

Other studies of hemorrhagic shock have shown that the fraction of cardiac output distributed to dermal, renal, and splanchnic beds declines, whereas the fraction distributed to brain and myocardium increases (20, 35), a phenomenon termed "centralization." The constriction of the resistance arteries may serve to sustain blood pressure, and constriction of the capacitance vessels may enhance blood redistribution from the skin to the vital organs. In summary, this study demonstrates the central role of resistance arteries in reducing blood flow in hemorrhagic shock and resuscitation, a phenomenon that has a significant impact on peripheral vascular resistance and may contribute to the blood centralization.

The authors acknowledge the contribution of Dr. Shunichi Usami for evaluating the viscometry data and Dr. Dominique Erni for suggesting the surgical technique.

This work has been supported in part by a National Heart, Lung, and Blood Institute Program Project (HL-48018); Grants-in-Aid for Scientific Research from the Ministry of Education, Science, Sports and Culture, Japan (07508005); and Health Science Research Grants (Artificial Blood Project) from the Ministry of Health and Welfare, Japan. H. Sakai was an overseas research fellow of the Japan Society for the Promotion of Science (1996–1997) and is a research resident of the Japan Health Sciences Foundation (1998).

Addresses for reprint requests and correspondence: M. Intaglietta, Dept. of Bioengineering, University of California, San Diego, 9500 Gilman Dr., La Jolla, CA 92093-0412; E. Tsuchida, Dept. of Polymer Chemistry, Advanced Research Institute for Science and Engineering, Waseda Univ., Tokyo 169-8555.

Received 13 April 1998; accepted in final form 20 October 1998.

REFERENCES

1. **Boegehold, M. A., and P. C. Johnson.** Periarteriolar and tissue P_{O_2} during sympathetic escape in skeletal muscle. *Am. J. Physiol.* 254 (*Heart Circ. Physiol.* 23): H929–H936, 1988.
2. **Bohlen, H. G.** Localization of vascular resistance changes during hypertension. *Hypertension* 8: 181–183, 1986.
3. **Colantuoni, A., S. Bertuglia, and M. Intaglietta.** Microvessel diameter changes during hemorrhagic shock in unanesthetized hamsters. *Microvasc. Res.* 30: 133–142, 1985.
4. **Davis, M. J.** Control of bat wing capillary pressure and blood flow during reduced perfusion pressure. *Am. J. Physiol.* 255 (*Heart Circ. Physiol.* 24): H1114–H1129, 1988.
5. **Davis, M. J., P. N. Ferrer, and R. W. Gore.** Vascular anatomy and hydrostatic pressure profile in the hamster cheek pouch. *Am. J. Physiol.* 250 (*Heart Circ. Physiol.* 19): H291–H303, 1986.
6. **Duling, B. R.** The role of the resistance arteries in the control of peripheral resistance. In: *Resistance Arteries: Structure and Function*, edited by M. J. Mulvany, C. Aalkjær, A. M. Heagerty, N. C. B. Nyborg, and S. Strandgraard. Oxford, UK: Elsevier Science, 1991, p. 3–9.
7. **Endrich, B., K. Asaishi, A. Götz, and K. Messmer.** Technical report–a new chamber technique for microvascular studies in unanesthetized hamsters. *Res. Exp. Med. (Berl.)* 177: 125–134, 1980.
8. **Erni, D. H. Sakai, A. G. Tsai, A. Banic, and M. Intaglietta.** The hamster island flap–a versatile model for investigating ischemia due to trauma and surgery by intravital microscopy (Abstract). *J. Vasc. Res.* 35, *Suppl.* 2: 74, 1998.
9. **Faber, J. E.** In situ analysis of α-adrenoreceptors on arteriolar and venular smooth muscle in rat skeletal muscle microcirculation. *Circ. Res.* 62: 37–50, 1988.
10. **Fenger-Gron, J., M. J. Mulvany, and K. L. Christensen.** Intestinal blood flow is controlled by both feed arteries and microcirculatory resistance vessels in freely moving rats. *J. Physiol. (Lond.)* 498: 215–224, 1997.
11. **Griffith, T. M., D. H. Edwards, R. L. Davies, and A. H. Henderson.** The role of EDRF in flow distribution: a microangiographic study of the rabbit isolated ear. *Microvasc. Res.* 37: 162–177, 1989.
12. **Hirata, S., and I. Ninomiya.** Nonuniform effects of sympathetic nerve and α-receptor blockade on internal diameter of small arteries in the rabbit ear. *Clin. Hemorheol.* 2: 229–241, 1982.
13. **Intaglietta, M., P. C. Johnson, and R. M. Winslow.** Microvascular and tissue oxygen distribution. *Cardiovasc. Res.* 32: 632–643, 1996.
14. **Intaglietta, M., N. R. Silverman, and W. R. Tompkins.** Capillary flow velocity measurements in vivo and in situ by television methods. *Microvasc. Res.* 10: 165–179, 1975.
15. **Intaglietta, M., and W. R. Tompkins.** Microvascular measurements by video image shearing and splitting. *Microvasc. Res.* 5: 309–312, 1973.
16. **Johnson, P. C.** The myogenic response. *News Physiol. Sci.* 6: 41–42, 1991.
17. **Kerger, H., D. J. Saltzman, M. D. Menger, K. Messmer, and M. Intaglietta.** Systemic and subcutaneous microvascular oxygen tension dissociation during 4-h hemorrhagic shock in conscious hamsters. *Am. J. Physiol.* 270 (*Heart Circ. Physiol.* 39): H827–H836, 1996.
18. **Kerger, H., I. P. Torres Filho, M. Rivas, R. M. Winslow, and M. Intaglietta.** Systemic and subcutaneous microvascular oxygen tension in conscious Syrian golden hamsters. *Am. J. Physiol.* 268 (*Heart Circ. Physiol.* 37): H802–H810, 1995.
19. **Kerger, H., A. G. Tsai, D. J. Saltzman, R. M. Winslow, and M. Intaglietta.** Fluid resuscitation with oxygen versus nonoxygen

carriers after 2-h hemorrhagic shock in conscious hamsters. *Am. J. Physiol.* 272 (*Heart Circ. Physiol.* 41): H525–H537, 1997.

20. **Koehler, R. C., R. J. Traystman, and M. D. Johnes, Jr.** Regional blood flow and O_2 transport during hypoxic and CO hypoxia in neonatal and adult sheep. *Am. J. Physiol.* 248 (*Heart Circ. Physiol.* 17): H118–H124, 1985.
21. **Koller, A., D. Sun, and G. Kaley.** Role of shear stress and endothelial prostaglandins in flow- and viscosity induced dilation of arterioles in vivo. *Circ. Res.* 72: 1276–1284, 1993.
22. **Kreimeier, U., U. B. Bruuckner, S. Niemczyk, and K. Messmer.** Hypertonic saline dextran for resuscitation from traumatic hemorrhagic hypotension: effect on regional blood flow. *Circ. Shock* 32: 83–99, 1990.
23. **Leech, C. J., and J. E. Faber.** Differential sensitivity of venular and arteriolar α-adrenergic receptor constriction to inhibition by hypoxia: role of receptor subtype and coupling heterogeneity. *Circ. Res.* 78: 1064–1074, 1996.
24. **Lipowsky, H., and B. Zweifach.** Application of the "two-slit" photometric technique to the measurement of microvascular volumetric flow rates. *Microvasc. Res.* 15: 93–101, 1978.
25. **Lombard, J. H., R. P. Kaminski, and W. J. Stekiel.** Arteriolar responses to changes in oxygen availability following single withdrawal hemorrhage. *Microvasc. Res.* 21: 332–342, 1981.
26. **McGillivray-Anderson, K. M., and J. E. Faber.** Effect of acidosis on contraction of microvascular smooth muscle by α_1- and α_2-adrenoreceptors. Implications for neural and metabolic regulation. *Circ. Res.* 66: 1643–1657, 1990.
27. **Meininger, G. A., K. L. Fehr, and M. B. Yates.** Anatomic and hemodynamic characteristics of the blood vessels feeding the cremaster skeletal muscle in the rat. *Microvasc. Res.* 33: 81–97, 1987.
28. **Mulvany, M. J., C. Aalkjær, A. M. Heagerty, N. C. B. Nyborg, and S. Strandgraard** (Editors). *Resistance Arteries: Structure and Function*. Oxford, UK: Elsevier Science, 1991.
29. **Nolte, D., A. Botzlar, S. Pickelmann, E. Bouskela, and K. Messmer.** Effects of diaspirin-crosslinked hemoglobin (DCLHb) on the microcirculation of striated skin muscle in the hamster: a study on safety and toxicity. *J. Lab. Clin. Med.* 130: 314–327, 1997.
30. **O'Brien, J. J., Jr., E. C. Lucey, and G. L. Sinder.** Arterial blood gases in normal hamsters at rest and during exercise. *J. Appl. Physiol.* 46: 806–810, 1979.
31. **Papenfuss, H. D., J. F. Gross, M. Intaglietta, and F. A. Treese.** A transparent access chamber for the rat dorsal skin fold. *Microvasc. Res.* 18: 311–318, 1979.
32. **Pascual, J. M. S., D. E. Runyon, J. C. Watson, C. B. Clifford, M. A. Dubick, and G. C. Kramer.** Resuscitation of hypovolemia in pigs using near saturated sodium chloride solution in dextran. *Circ. Shock* 40: 115–124, 1993.
33. **Pohl, U., K. Herlan, A. Huang, and E. Bassenge.** EDRF-mediated shear-induced dilation opposes myogenic vasoconstriction in small rabbit arteries. *Am. J. Physiol.* 261 (*Heart Circ. Physiol.* 30): H2016–H2023, 1991.
34. **Sakai, H., A. G. Tsai, H. Kerger, S. I. Park, S. Takeoka, H. Nishide, E. Tsuchida, and M. Intaglietta.** Subcutaneous microvascular responses to hemodilution with red cell substitutes consisting of polyethyleneglycol-modified vesicles encapsulating hemoglobin. *J. Biomed. Mater. Res.* 40: 66–78, 1998.
35. **Schlichtig, R., D. J. Kramer, and M. R. Pinsky.** Flow redistribution during progressive hemorrhage is a determinant of a critical O_2 delivery. *J. Appl. Physiol.* 70: 169–178, 1991.
36. **Sehgal, S. S., and B. R. Duling.** Communication between feed arteries and microvessels in hamster striated muscle: segmental vascular responses are functionally coordinated. *Circ. Res.* 59: 283–290, 1986.
37. **Slaaf, D. W., R. S. Reneman, and C. A. Wiederhielm.** Pressure regulation in muscle of unanesthetized bats. *Microvasc. Res.* 33: 315–326, 1987.
38. **Smiesko, V., D. J. Lang, and P. C. Johnson.** Dilator response of rat mesenteric arcading arterioles to increased blood flow velocity. *Am. J. Physiol.* 257 (*Heart Circ. Physiol.* 26): H1958–H1965, 1989.
39. **Torres, Filho, I. P., M. A. Boegehold, E. Bouskela, S. D. House, and P. C. Johnson.** Microcirculatory responses in cat sartorius muscle to hemorrhagic hypotension. *Am. J. Physiol.* 257 (*Heart Circ. Physiol.* 26): H1647–H1655, 1989.
40. **Torres, Filho, I. P., and M. Intaglietta.** Microvascular P_{O_2} measurements by phosphorescence decay method. *Am. J. Physiol.* 265 (*Heart Circ. Physiol.* 34): H1434–H1438, 1993.
41. **Tsai, A. G., B. Friesenecker, M. C. Mazzoni, H. Kerger, D. G. Buerk, P. C. Johnson, and M. Intaglietta.** Microvascular and tissue oxygen gradients in the rat mesentery. *Proc. Natl. Acad. Sci. USA* 95: 6590–6595, 1998.
42. **Usami, S., W. Reinhart, S. Danoff, and S. Chen.** A new capillary viscometer for measurements on small blood samples over a wide shear rate range. *Clin. Hemorheol.* 4: 295–297, 1984.
43. **Whitmore, R. L.** *Rheology of the Circulation*. Oxford, UK: Pergamon, 1968.
44. **Williams, D. A., and S. S. Segal.** Feed artery role in blood flow control to rat hindlimb skeletal muscle. *J. Physiol. (Lond.)* 463: 631–646, 1993.
45. **Wit, C., C. Schäfer, P. Bismarck, S.-S. Bolz, and U. Pohl.** Elevation of plasma viscosity induces sustained NO-mediated dilation in the hamster cremaster microcirculation in vivo. *Pflügers Arch.* 434: 354–361, 1997.
46. **Zhao, K.-S., D. Junker, F. A. Delano, and B. W. Zweifach.** Microvascular adjustments during irreversible hemorrhagic shock in rat skeletal muscle. *Microvasc. Res.* 30: 143–153, 1985.